

Environmental Science Water Research & Technology

Accepted Manuscript

This article can be cited before page numbers have been issued, to do this please use: F. Mohamadi, T. Chen, R. Hofmann and C. Wang, *Environ. Sci.: Water Res. Technol.*, 2026, DOI: 10.1039/D6EW00171H.



This is an Accepted Manuscript, which has been through the Royal Society of Chemistry peer review process and has been accepted for publication.

Accepted Manuscripts are published online shortly after acceptance, before technical editing, formatting and proof reading. Using this free service, authors can make their results available to the community, in citable form, before we publish the edited article. We will replace this Accepted Manuscript with the edited and formatted Advance Article as soon as it is available.

You can find more information about Accepted Manuscripts in the [Information for Authors](#).

Please note that technical editing may introduce minor changes to the text and/or graphics, which may alter content. The journal's standard [Terms & Conditions](#) and the [Ethical guidelines](#) still apply. In no event shall the Royal Society of Chemistry be held responsible for any errors or omissions in this Accepted Manuscript or any consequences arising from the use of any information it contains.

This study evaluated uncertainties in the external calibration method for hydroxyl radical scavenging capacity (HRSC) measurement. Methylene blue was confirmed as a suitable hydroxyl radical probe, and interferences from carbonate radical, superoxide, and singlet oxygen were negligible. Overall, the results validate external calibration as a robust approach for HRSC monitoring and cost-effective optimization of advanced oxidation processes.

[View Article Online](#)

DOI: 10.1039/D6EW00171H



1 Evaluating Interferences in the External Calibration Method for 2 Hydroxyl Radical Scavenging Capacity Measurement

3
4 Fateme Mohamadi¹, Tianyi Chen², Ron Hofmann², Chengjin Wang^{1*}

5
6 ¹Department of Civil Engineering, University of Manitoba, 15 Gillson St., Winnipeg, Manitoba
7 R3T 5V6, Canada

8 ²Department of Civil and Mineral Engineering, University of Toronto, 35 St. George Street,
9 Toronto, Ontario M5S 1A4, Canada.

10
11 *Corresponding author:

12 Chengjin Wang, Ph.D., P.Eng.

13 Dept. Civil Engineering, University of Manitoba

14 15 Gillson St., Winnipeg, Manitoba, Canada R3T 5V6

15 Tel.: 204-474-8381

16 Email: chengjin.wang@umanitoba.ca

17

18



Abstract

19 In most advanced oxidation processes (AOPs), hydroxyl radical ($\bullet\text{OH}$) is produced to transform
20 micropollutants. However, it can also be consumed by non-target compounds including organic
21 and some inorganic matter, known as $\bullet\text{OH}$ scavengers. The pseudo-first order consumption rate of
22 $\bullet\text{OH}$ is termed as the hydroxyl radical scavenging capacity (HRSC). HRSC directly influences
23 AOP performance, which is a crucial parameter for AOP design and operation. An external
24 calibration method has been developed to measure HRSC, using methylene blue (MB) as the probe
25 compound. This method assumes that MB only reacts with $\bullet\text{OH}$, but experimental investigation is
26 needed to confirm this. In this study, MB decay was monitored under reaction conditions featuring
27 high concentrations of superoxide radical, organic radical, carbonate radical, and singlet oxygen.
28 The results showed that these reactive species did not contribute to MB decay. Additionally, as
29 chloride, bromide, and chloramines may introduce new reactive species through UV photolysis or
30 reaction with $\bullet\text{OH}$, their impacts on HRSC measurement were investigated. Our results show that
31 chloride has no impact on HRSC, while bromide at low mg/L levels significantly increases it.
32 Chloramines were found to significantly increase HRSC. Our findings confirm that the external
33 calibration method is reliable for most drinking water samples due to the negligible interferences
34 from non- $\bullet\text{OH}$ species. For water samples containing chloramines, a protocol was developed to
35 measure background HRSC with chloramines quenched using sodium sulfite. This approach
36 assumes that the contribution of chloramines can be modeled when their concentrations are
37 accurately determined.

38 Keywords: Hydroxyl Radical, Methylene Blue, Advanced Oxidation, Chloramine, Superoxide,
39 Singlet Oxygen, Carbonate Radical.



40

41 **1. Introduction**

42 Advanced oxidation processes (AOPs) generate the hydroxyl radical ($\bullet\text{OH}$), which is a strong
43 oxidant reacting with numerous species in water. Although $\bullet\text{OH}$ is typically used to oxidize
44 micropollutants, it can also be scavenged by non-target compounds (e.g., natural organic matter
45 and bicarbonate).¹ This scavenging effect decreases the concentration of available $\bullet\text{OH}$ to destroy
46 the target contaminants, therefore it is useful to determine the extent of water scavenging to guide
47 AOP design and operation. Quantitatively, the hydroxyl radical scavenging capacity (HRSC) is
48 the sum of the pseudo first-order consumption rates of $\bullet\text{OH}$ by non-target compounds in a water
49 sample, which is the sum of each scavenger's molar concentration $[\text{S}_i]$ (M) multiplied by its
50 second-order reaction rate constant k_i ($\text{M}^{-1}\cdot\text{s}^{-1}$) in $\bullet\text{OH}$ reactions (Eq. 1).

$$\text{HRSC} = \sum k_i [\text{S}_i] \quad (\text{Eq. 1})$$

51 The HRSC of a water sample with known constituents and known hydroxyl reaction rates can be
52 calculated with Eq.1. However, the concentration and reactivity of individual $\bullet\text{OH}$ -consuming
53 constituents in most water samples are unknown, necessitating the development of an experimental
54 method to directly measure the HRSC. Therefore, an external calibration method was developed
55 for HRSC measurement, which significantly simplified the test procedure and shortened the testing
56 time compared to conventional methods.²

57 In the external calibration method, fixed amounts of methylene blue (MB) and H_2O_2 are added to
58 standard solutions with known scavenging capacities. The solutions are then exposed to a fixed
59 UV fluence, which photolyzes H_2O_2 to generate $\bullet\text{OH}$ at a constant rate. The MB decay rate in each
60 solution, which is inversely related to the solution's HRSC, is monitored using a



61 spectrophotometer. A calibration curve relating hydroxyl radical scavenging capacity (HRSC) to
62 MB decay rate is established from these standards. Under identical UV/H₂O₂ conditions, MB
63 decay in samples with unknown HRSC is measured and the resulting decay rates are converted to
64 HRSC values using the calibration curve.

65 This method assumes that the colour loss due to MB decay is only attributed to the reaction
66 between hydroxyl radical and MB. However, during UV/H₂O₂ reaction in a water sample, there
67 are reactive species generated other than •OH, such as the carbonate radical (CO₃•⁻),³ various
68 organic radicals,⁴ superoxide radical (O₂•⁻),⁵ and singlet oxygen (¹O₂).⁶ If these species react with
69 MB, the resulting measurement is not representative of solely •OH scavenging, and the MB decay
70 rate would be accelerated and the measured HRSC would be falsely overestimated. Furthermore,
71 the external calibration method has not been tested in the water reuse scenario, especially for
72 reverse osmosis (RO) permeate containing chloramines. The RO permeate is expected to have low
73 HRSC due to low concentrations of total organic carbon (TOC) (<0.5 mg/L as C) and inorganic
74 carbon (<15 mg/L as CaCO₃),⁷ but the permeate usually contains residual chloramines applied
75 upstream for membrane fouling control.⁸ Chloramines contribute to HRSC through their reactions
76 with •OH but they can also generate •OH due to UV photolysis. This may introduce errors to the
77 external calibration method by invalidating the constant •OH generation assumption. Additionally,
78 the impact of chloride (Cl⁻) and bromide (Br⁻) on HRSC measurement has not been reported.
79 Chloride and bromide have the potential to react with •OH and produce secondary or tertiary
80 reactive species such as Cl₂•⁻, ClOH•⁻, Br₂•⁻, and BrOH•⁻.⁹ The reactivity of these halogen-
81 containing radicals toward MB and their impact on HRSC measurement remain unknown.

82 To address the uncertainties associated with the external calibration method, this study was
83 designed to (1) test the reactivity of MB towards superoxide radicals, organic radicals, carbonate



84 radicals, and singlet oxygen under conditions featuring high concentrations of each of these
85 reactive species, (2) measure the HRSC of synthetic RO samples with and without quenching
86 chloramines, and (3) compare the impact of chloride and bromide on the $\bullet\text{OH}$ scavenging capacity
87 measurement.

88 2. Materials and methods

89 2.1 Chemicals and materials

90 All chemicals used in this study were ACS grade unless otherwise specified. Methylene blue
91 hydrate powder (92%) and hydrogen peroxide (30% w/w) were purchased from Sigma-Aldrich
92 and used to prepare 1 g/L MB stock solution and 10 g/L H_2O_2 stock solution respectively.
93 Isopropyl alcohol, furfuryl alcohol, benzoic acid, nitrobenzene, sodium sulfite, sodium carbonate,
94 and sodium bisulfite were also sourced from Sigma-Aldrich. Acetone (NF FCC grade), phenol,
95 methanol (HPLC grade), ethanol and acetic acid were purchased from Fisher Scientific.
96 Acetonitrile was purchased from VWR Chemicals BDH. Humic acid derived from the Suwannee
97 River was obtained from the International Humic Substances Society.

98 A synthetic water matrix was prepared by diluting Winnipeg's tap water 15-fold with Milli-Q
99 water, resulting in a final TOC ≤ 0.3 mg-C/L and pH close to neutral. The free chlorine
100 concentration was always negligible before tests. This matrix was used for all test conditions
101 except the bromide and chloride effect tests, for which tap water was used directly (TOC: 4.3 mg-
102 C/L, Cl^- :~5 mg/L, Br^- :<0.05 mg/L, residual free chlorine: negligible before tests as it was quenched
103 by H_2O_2), and the singlet oxygen effect tests, for which Milli-Q water was used. When needed, pH
104 was adjusted using HCl or NaOH solutions. To avoid buffer interference with HRSC
105 measurements, no buffer was used for pH adjustment. The solution pH remained stable for several



106 minutes, sufficient to complete the HRSC measurement. The pH was monitored before and after
107 the HRSC measurement to confirm its short-term stability, remaining within ± 0.2 units. The
108 primary reason for preparing the synthetic water using diluted Winnipeg water was to simulate the
109 TOC level in the RO permeate for studying the effect of chloramines on HRSC measurement,
110 although it was also used in most of the other experiments.

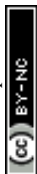
111 2.2 Generation of non- \bullet OH species

112 2.2.1 Carbonate radical ($\text{CO}_3^{\bullet-}$)

113 To produce carbonate radical ($\text{CO}_3^{\bullet-}$), 20 mM of sodium carbonate (2.2 g/L) was added to the 40
114 mL synthetic water sample in the presence of 1.47 mM (50 mg/L) hydrogen peroxide and 5 μM
115 MB, resulting in a pH of 10.8-11.0. The HRSC of carbonate at this pH would be around 6.2×10^6
116 s^{-1} (at an average pH of 10.9, approximately 80% of the added inorganic carbon is present as
117 carbonate, and the product of carbonate concentration and the rate constant $k = 3.9 \times 10^8 \text{ M}^{-1} \text{ s}^{-1}$ is
118 $6.2 \times 10^6 \text{ s}^{-1}$, neglecting the contribution from bicarbonate), more than 50 times higher than the
119 combined HRSC caused by the TOC, the spiked MB, and the H_2O_2 , which was approximately 1.0
120 $\times 10^5 \text{ s}^{-1}$ as estimated based on their concentrations and reactivities toward \bullet OH. Being exposed to
121 UV light generated using a collimated beam system (Fig. S1), almost all the generated hydroxyl
122 radicals were converted into $\text{CO}_3^{\bullet-}$ resulting in a high concentration of $\text{CO}_3^{\bullet-}$ and a very low amount
123 of hydroxyl radicals. Under this condition, if the decay rate of methylene blue was negligible, it
124 would indicate the negligible contribution of carbonate radicals to methylene blue degradation.

125 2.2.2 Organic radicals

126 Similarly, methylene blue decay was monitored under conditions when organic radicals were the
127 dominant reactive species in synthetic water samples. Such conditions were achieved by applying



128 organic compounds at concentrations high enough to convert almost all the hydroxyl radicals into
 129 organic radicals. The organic compounds tested in this study ranged from simple structure
 130 molecules (e.g., ethanol) to complex molecules (e.g., humic acids) with different functional groups
 131 (e.g., hydroxyl, carboxylate, and nitrile) and reactivities to investigate various organic radicals
 132 which might be present in UV/H₂O₂ process, including carbon centered radicals such as methyl
 133 radicals, oxygen-centered radicals such as alkoxy radicals, and others. The tested organic
 134 compounds and their concentrations are listed in Table 1, along with their contribution to HRSC.
 135 As shown in Table 1, the spiked organic matter exhibited sufficient HRSC to consume nearly all
 136 of the hydroxyl radicals and generate various organic radicals. Each compound's impact on MB
 137 decay was evaluated individually in the presence of 50 mg/L H₂O₂ and 5 μM methylene blue (MB).
 138 Furthermore, a solution of 150 mg-C/L (approximately 13 mM as C) humic acid from Suwannee
 139 River from the International Humic Substances Society was prepared to be tested as a
 140 representation of natural organic matter (NOM).

141 Table 1: Expected HRSC caused by tested organic species

Organic Compound	Hydroxyl Rate Constant (M ⁻¹ s ⁻¹)	Molar Concentration (M)	Expected HRSC (s ⁻¹)
Isopropyl alcohol (IPA)	1.9×10^9 ¹¹	0.65	1.9×10^9
Methanol	9.0×10^8 ¹¹	0.70	6.8×10^8
Phenol	6.0×10^9 ¹¹	0.11	6.5×10^8
Acetate	8.5×10^7 ¹²	0.10	6.8×10^7
Acetonitrile	2.0×10^7 ¹¹	0.25	1.1×10^7
Ethanol	1.9×10^9 ¹¹	0.01	2.0×10^7

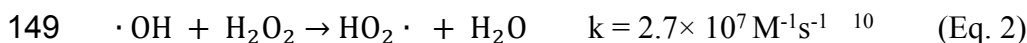


Acetone	1.0×10^8 ¹¹	0.27	2.9×10^7
Humic acid	3.0×10^8 ¹³	~ 0.013 (as C)	4.0×10^6

142

143 2.2.3 Superoxide radical ($O_2^{\cdot-}$).

144 Another common radical in UV/ H_2O_2 is superoxide ($O_2^{\cdot-}$). Hydrogen peroxide is a generator of
 145 $\cdot OH$ under UV exposure, and at the same time, it also consumes $\cdot OH$ as described in Eqs. 2 and 3.
 146 When the HRSC caused by hydrogen peroxide is higher than any other species in the water matrix,
 147 $\cdot OH$ is mainly consumed by H_2O_2 and generates superoxide radical. This means that at high
 148 concentrations of hydrogen peroxide, superoxide radical can be dominant.



151 To investigate the contribution of superoxide radicals towards MB decay, benzoic acid (BA) and
 152 nitrobenzene (NB), along with MB, were applied to synthetic water as $\cdot OH$ probe compounds.
 153 While NB and BA are reported to be reactive towards hydroxyl radicals, they have no reactivity
 154 towards superoxide radicals.¹⁴ The degradations of BA, NB, and MB, all with an initial
 155 concentration of 5 μM , were monitored at different H_2O_2 concentrations under UV as described
 156 below. The first-order decay rates of MB, BA, and NB were calculated as k'_{MB} , k'_{BA} , and k'_{NB} . If
 157 the ratio of k_{MB}/k_{BA} or k_{MB}/k_{NB} was constant at different concentrations of hydrogen peroxide, it
 158 means that hydroxyl radical is the only contributor to MB decay as shown in Eq. 4 (using BA as
 159 an example).

$$160 \frac{k'_{MB}}{k'_{BA}} = \frac{k_{MB}[\cdot OH]_{ss}}{k_{BA}[\cdot OH]_{ss}} = \frac{k_{MB}}{k_{BA}} \quad (Eq. 4)$$



161 where, $[\cdot\text{OH}]_{ss}$ is the steady-state concentration of hydroxyl radical, k_{MB} and k_{BA} are the second-
 162 order rate constants for oxidation reactions by $\cdot\text{OH}$. However, if $\text{O}_2^{\cdot-}$ contributes to MB decay,
 163 $\frac{k'_{MB}}{k'_{BA}}$ (or $\frac{k_{MB}}{k_{NB}}$) will depend on the hydrogen peroxide concentration, indicating that $\text{O}_2^{\cdot-}$ contribution
 164 is not negligible. In another words, if superoxide significantly reacts with MB, then $\frac{k'_{MB}}{k'_{BA}}$ will
 165 increase with the increase in the H_2O_2 concentration, as shown in Eq. 5 (using BA as an example):

$$166 \quad \frac{k'_{MB}}{k'_{BA}} = \frac{k_{MB}[\cdot\text{OH}]_{ss} + k_{MB/\text{O}_2^{\cdot-}}[\text{O}_2^{\cdot-}]_{ss}}{k_{BA}[\cdot\text{OH}]_{ss}} \quad (\text{Eq. 5})$$

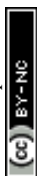
167 where, $[\text{O}_2^{\cdot-}]_{ss}$ is the steady-state concentration of superoxide radical which increases with the
 168 H_2O_2 concentration, and $k_{MB/\text{O}_2^{\cdot-}}$ is the second-order rate constant for reaction between MB and
 169 $\text{O}_2^{\cdot-}$. Therefore, by using a wide range of H_2O_2 concentrations (from 10 mg/L to 2,000 mg/L),
 170 different concentrations of $\text{O}_2^{\cdot-}$ can be generated, at which the degradation of MB, BA, and NB
 171 were monitored.

172 2.2.4 Singlet oxygen ($^1\text{O}_2$)

173 To generate singlet oxygen, hydrogen peroxide and sodium hypochlorite were added to Milli-Q
 174 water to produce singlet oxygen (Eq 6),¹⁵ and the Milli-Q water matrix was used to minimize
 175 background consumption of $^1\text{O}_2$.



177 To confirm the presence of singlet oxygen at sufficient concentrations for micropollutant
 178 degradation, furfuryl alcohol (FFA), a known probe for singlet oxygen, was used.¹⁶ Experiments
 179 were conducted by adding hydrogen peroxide and sodium hypochlorite at a 1:1 molar ratio to a
 180 solution containing approximately 5 μM FFA. The decay of FFA was monitored to confirm the
 181 generation of $^1\text{O}_2$. Reaction conditions were varied with OCl^- and H_2O_2 concentrations of 1, 2, and



182 3 mM at room temperature. Reactions were carried out in batch glass reactors containing 100 mL
183 of deionized water, equipped with a magnetic stirrer. The duration of each treatment was 5 min,
184 and samples were collected immediately after that for FFA analysis as described later.

185 2.3 Investigating chloride and bromide impact

186 To investigate the effect of chloride on HRSC, sodium chloride (NaCl) was added to the tap water
187 samples to create concentration ranges from 0 mg/L to 200 mg/L as Cl⁻. Similarly, the effect of
188 bromide was tested on HRSC measurement by adding potassium bromide (KBr) to create different
189 concentrations of Br⁻ from 0 mg/L to 2 mg/L. The HRSC of each sample was measured and
190 compared with the scavenging capacity of the water matrix before the halide ion additions.

191 2.4 Impact of chloramines

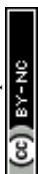
192 The impact of chloramines on HRSC measurement was investigated by adding different
193 concentrations of chloramines (0 to 12 mg/L as Cl₂) to the synthetic water with pH adjusted to 5.5
194 using HCl solution (i.e. simulated RO). The samples were then subjected to HRSC analysis using
195 the same method as described above. We then explored methods to quench chloramines prior to
196 HRSC measurement, using sulfite and bisulfite as quenching agents. This was done to determine
197 whether the quenching process could restore the HRSC to baseline values observed before
198 chloramine addition. The quenching process is usually necessary when water samples are shipped
199 to off-site laboratories for baseline HRSC analysis. Additional details on chloramine quenching
200 are provided in SI and Fig. S2.

201 2.5 Analytical methods



202 pH was measured using an Orion Star A211 benchtop pH meter (Thermo Scientific, Waltham,
203 Massachusetts, USA), and TOC was analyzed using a TOC-L_{CPH/CPN} analyzer (Shimadzu
204 Corporation, Kyoto, Japan). The decay of methylene blue was monitored using a VWR V-1200
205 spectrophotometer (Radnor, Pennsylvania, USA) at MB's signature wavelength of 664 nm. The
206 pseudo-first-order decay rate of MB was calculated based on the change in absorbance (A) over
207 time. H₂O₂ concentrations were determined using the triiodide method, which is based on a
208 reaction between H₂O₂ and potassium iodide (KI) in the presence of ammonium molybdate as a
209 catalyst in a buffered solution.¹⁷ The DPD colorimetric method was used to measure free and total
210 chlorine in water samples.¹⁸ Concentrations of nitrobenzene, benzoic acid and furfuryl alcohol
211 were determined using an Alliance High-performance liquid chromatography (HPLC)-UV system
212 equipped with a 2998 photodiode array (PDA) UV detector (Waters Corporation, Milford,
213 Massachusetts, USA). A Symmetry® C₁₈ reversed-phase column (3.5 µm particle size, 4.6 × 150
214 mm; Waters Corporation, Milford, Massachusetts, USA) was used for separation. The mobile
215 phase comprised A (methanol) and B (10% methanol in water, pH 4 adjusted using phosphoric
216 acid). Gradient elution ran from 30%A/70%B to 70%A/30%B and returned to 30%A/70%B. The
217 peaks associated with the compounds were monitored at 230 nm.

218 Statistical analysis was performed to investigate the significance of differences in MB decay rates
219 between direct photolysis and conditions in the presence of other radicals. The degradation rate of
220 MB (k) under each condition was determined from the slope of the corresponding decay curve.
221 Statistical comparisons of the k values were performed between each experimental condition and
222 the control condition (i.e. MB direct photolysis). A two-tailed unpaired Student's t-test with
223 unequal variances was applied using Microsoft Excel. Differences were considered statistically
224 significant at $p < 0.05$.



225 3. Results and discussion

226 3.1 Reactivities of non-•OH species with MB

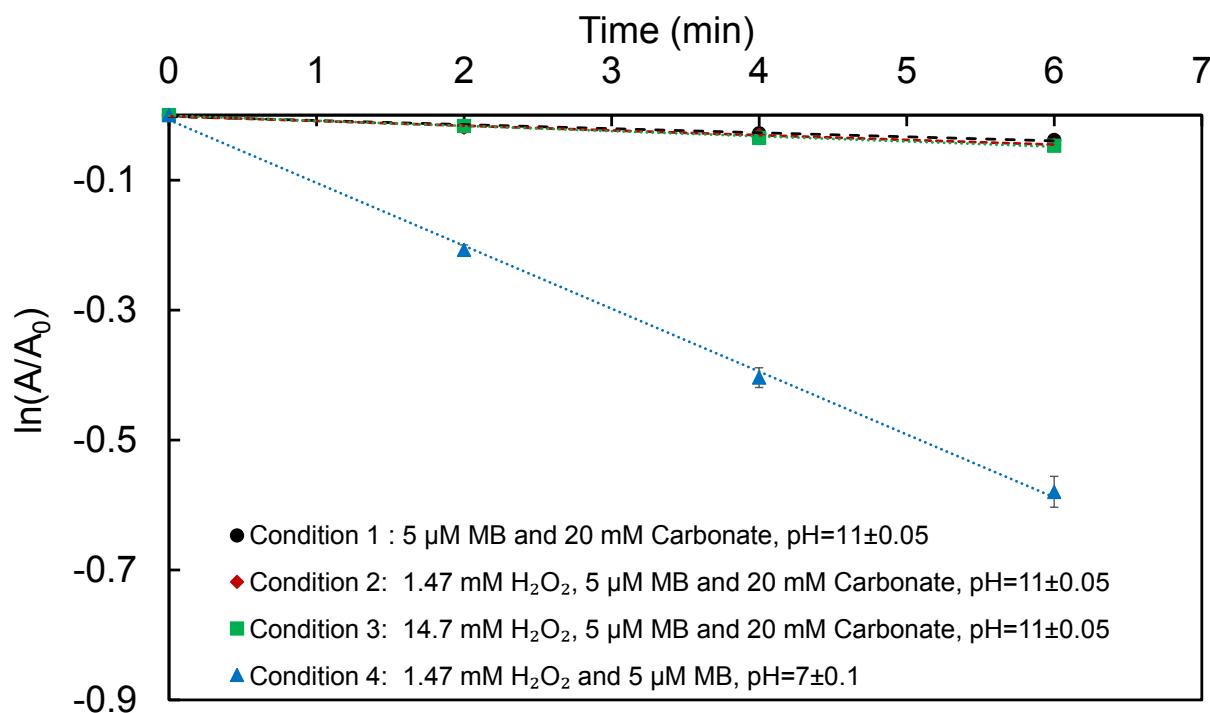
227 The potential interference of carbonate radicals, organic radicals, superoxide radicals, and singlet
228 oxygen was evaluated to determine their contributions to MB decay. As detailed in the following
229 sections, none of the tested radicals exhibited any reaction with MB.

230 3.1.1 Carbonate radicals

231 Fig. 1 shows that the decay of MB in the presence of high concentrations of carbonate radical—
232 generated by quenching hydroxyl radicals with excess carbonate—is identical to that observed
233 during MB direct photolysis (i.e., no radical formation), as confirmed by the statistical analysis in
234 Table S1. For comparison, the figure also includes the MB decay profile under typical UV/H₂O₂
235 conditions without elevated carbonate levels, which displays a substantially faster decay rate. This
236 shows negligible contribution of carbonate radicals to the MB decay rate under the conditions
237 relevant to HRSC measurement (e.g., few minutes' reaction time, tens of mg/L of H₂O₂ under a
238 low-pressure mercury UV lamp). Notably, MB decay remained negligible when the H₂O₂
239 concentration was increased tenfold to 14.7 mM (500 mg/L), a condition expected to generate
240 much higher concentrations of carbonate radicals in the presence of excess carbonate. This can be
241 explained by the selective nature of CO₃^{•-} as an oxidant, targeting mainly electron-rich species
242 such as those with containing N-heterocycles, reductive sulfur species, phenols, and anilines.¹⁹
243 Although $k_{\text{CO}_3^{\bullet-}}$, the second order rate constants for carbonate radical reactions, as high as 10⁸-10⁹
244 M⁻¹s⁻¹ have been reported for some anilines (e.g. N-ethyl-aniline), MB is expected to exhibit much
245 lower rate constants because the lone pair on its nitrogen is delocalized over an extended aromatic
246 π -system, leaving no localized electron-rich moieties available for rapid electron transfer to CO₃^{•-}.



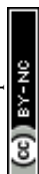
247 However, a detailed mechanistic study is needed to explain the low reactivity, if any, between MB
248 and carbonate radical.



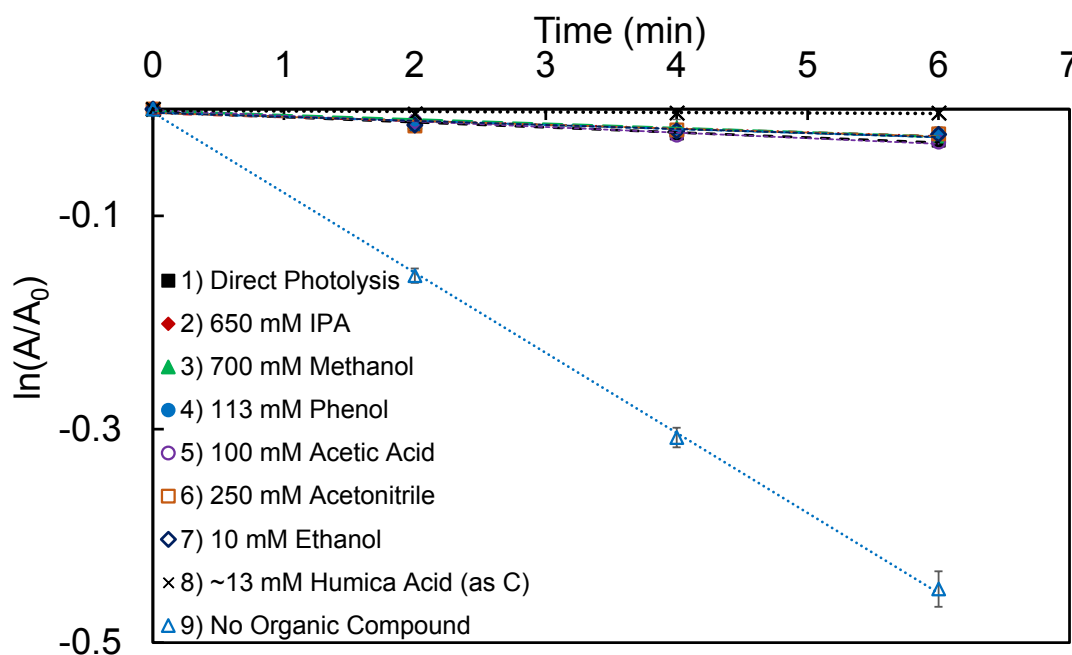
249
250 Fig. 1 Absorbance decrease in the 5 μM MB at 664 nm under direct photolysis (Condition 1), in
251 the presence of carbonate radical (Conditions 2 and 3) and hydroxyl radical (Condition 4). Tests
252 were conducted in synthetic water with initial TOC < 0.3 mg-C/L at room temperature. All Tests
253 were in triplicate, and error bars show the standard deviation.

255 3.1.2 Organic radicals

256 Fig. 2 shows the decay of MB under UV/H₂O₂ in the presence of various organic radicals,
257 compared with MB decay during direct photolysis (i.e., no H₂O₂ and no spiked organic scavengers)
258 and with UV/H₂O₂ treatment conducted without adding excessive organic scavengers. Under all
259 conditions involving organic radicals, the MB decay rate was the same as or very close to its decay
260 rate under direct photolysis (see Table S2 for statistical analysis results), significantly lower than
261 MB decay in the presence of $\bullet\text{OH}$ when no organic compound was spiked (see the line with the



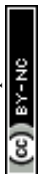
262 steep slope in Fig. 2). This indicates that the organic radicals generated from the reaction between
 263 hydroxyl radical and various organic compounds exhibited no measurable reactivity toward MB,
 264 confirming that the tested organic radicals do not interfere with in HRSC measurements when MB
 265 is used as the probe compound. This is not surprising, as most organic radicals—such as alkyl and
 266 alkoxy radicals—have much lower redox potentials than hydroxyl radicals. Most organic radicals
 267 tend to react with oxygen to form less reactive peroxy radicals or decompose into smaller organic
 268 species through self-decay or bimolecular reactions, rather than oxidizing MB.²⁰



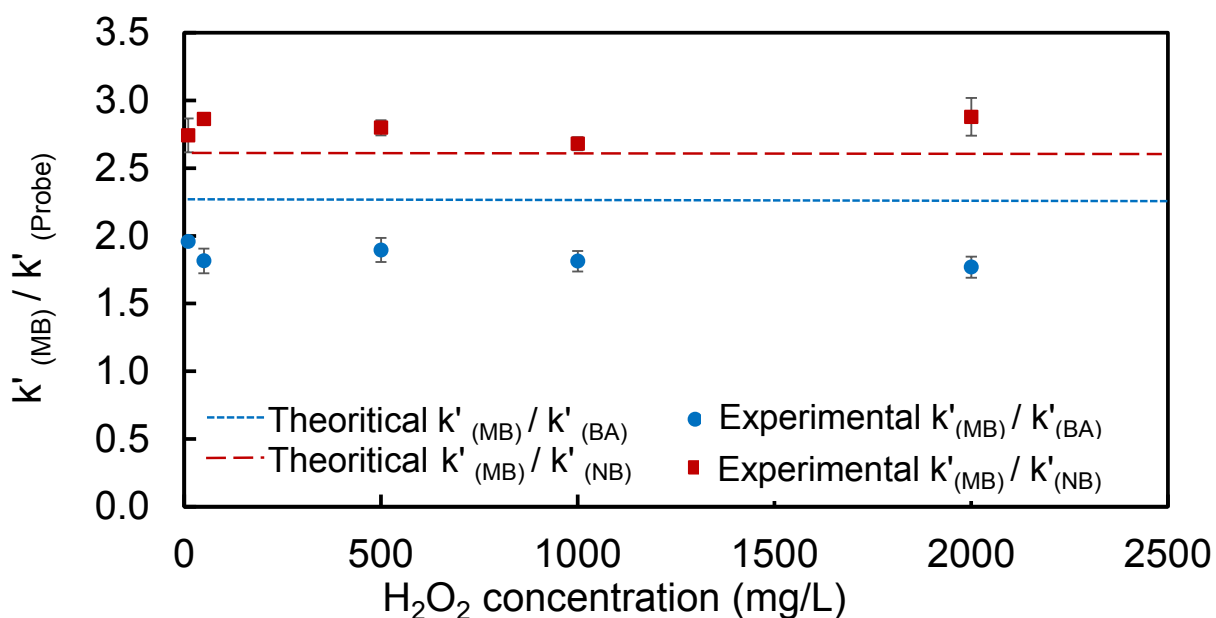
269
 270 Fig. 2 Absorbance decrease in the 5 μM MB at 664 nm in the presence of various organic
 271 radicals. $[\text{H}_2\text{O}_2]_0 = 1.47 \text{ mM}$ except for direct photolysis, and $\text{pH} = 7 \pm 0.2$. Tests were
 272 conducted in synthetic water with initial $\text{TOC} < 0.3 \text{ mg-C/L}$ at room temperature. All Tests were
 273 in triplicate, and error bars show the standard deviation. The parent compounds for the organic
 274 radicals are shown in the legend.

275

276 3.1.3 Superoxide radical



277 The decay of MB, BA, and NB was monitored under UV/H₂O₂ at different H₂O₂ doses, and their
 278 first-order rate constants were calculated and compared (Fig. 3). Specifically, the ratios of the MB
 279 decay rate (k'_{MB}) over NB decay rate (k'_{NB}) at different H₂O₂ concentrations (i.e., different
 280 superoxide concentrations) are plotted, along with the ratios of MB decay rate over BA decay rate
 281 (k'_{BA}). Fig. 3 shows that the two ratios remained consistent across a wide range of hydrogen
 282 peroxide concentrations (from 10 to 2,000 mg/L). This indicates that the superoxide radical does
 283 not react with MB at a detectable rate and thus does not interfere with HRSC measurements. This
 284 is consistent with many previous studies showing superoxide radical as a weak oxidant with
 285 negligible contributions in AOPs.^{5, 21}



286
 287 Fig. 3 Ratios of methylene blue (MB) decay rate to benzoic acid (BA) and nitrobenzene (NB)
 288 decay rate under UV exposure at different H₂O₂ doses. All tests were conducted in synthetic
 289 water at the room temperature. pH = 7 ± 0.2; [MB]₀ = [NB]₀ = [BA]₀ = 5 μM. The theoretical k'
 290 (MB) / k' (Probe), excluding contribution from superoxide radical, was calculated using rate
 291 constants reported for •OH with MB ($1.0 \times 10^{10} \text{ M}^{-1}\text{s}^{-1}$)²², NB ($3.9 \times 10^9 \text{ M}^{-1}\text{s}^{-1}$)¹¹ and BA ($4.3 \times$
 292 $10^9 \text{ M}^{-1}\text{s}^{-1}$)¹¹, respectively. The error bars indicate the maximum and minimum values from
 293 duplicate tests.

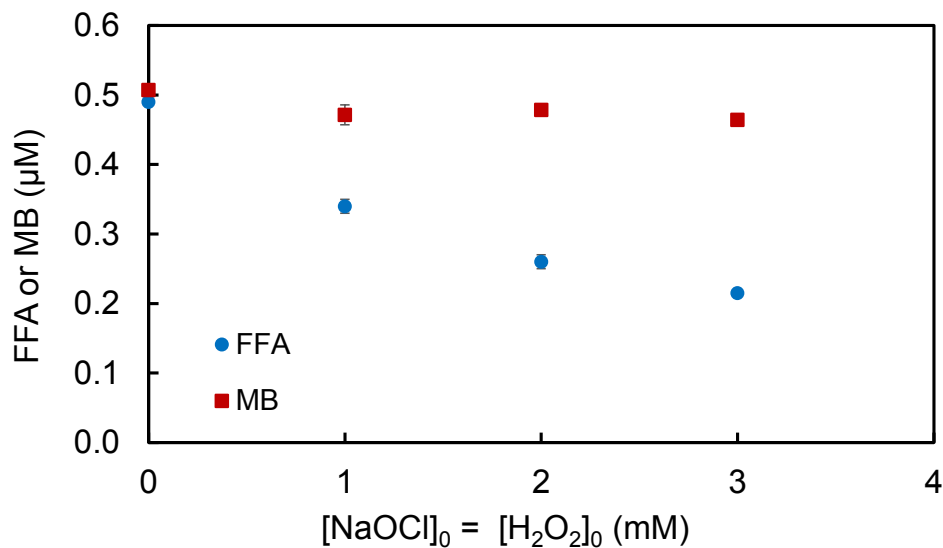
294



295 3.1.4 Singlet oxygen

296 Fig. 4 illustrates the degradation of furfuryl alcohol (FFA) after adding free chlorine and hydrogen
297 peroxide at various equimolar concentrations. When 1 mM of free chlorine and 1 mM of hydrogen
298 peroxide were added, the concentration of FFA decreased from 0.49 μM to 0.34 μM , accounting
299 for 31% removal. This removal was increased to 55% when the concentrations of chlorine and
300 peroxide were tripled. As FFA is a commonly used probe for singlet oxygen, the results confirmed
301 the effective generation of singlet oxygen through the reaction between chlorine and peroxide.²³
302 Fig. 4 also shows the decay of MB in the presence of singlet oxygen under the same conditions,
303 except that FFA was replaced with MB. The negligible change in MB concentration before and
304 after singlet oxygen generation, as indicated by the absorbance at 664 nm, confirms that singlet
305 oxygen does not contribute to MB degradation fast enough even in the efficient singlet oxygen
306 generating system (i.e., the classical chlorine-peroxide mixture). Considering that singlet oxygen
307 generation in the UV/H₂O₂ system occurs via secondary reactions and is less efficient than in the
308 NaOCl/H₂O₂ system, we further postulate that singlet oxygen's contribution to MB decay in the
309 HRSC measurements is negligible.



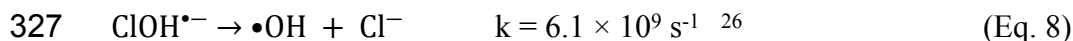


310
311 Fig. 4 Degradation of furfuryl alcohol (FFA) and methylene blue (MB) in Milli-Q water after
312 addition of NaOCl and H₂O₂ with 1:1 molar ratio to generate singlet oxygen at room temperature
313 and pH = 7.4±0.1. The error bars indicate the maximum and minimum values from duplicate
314 tests.

316 3.2 Effect of chloride and bromide on •OH scavenging capacity measurement

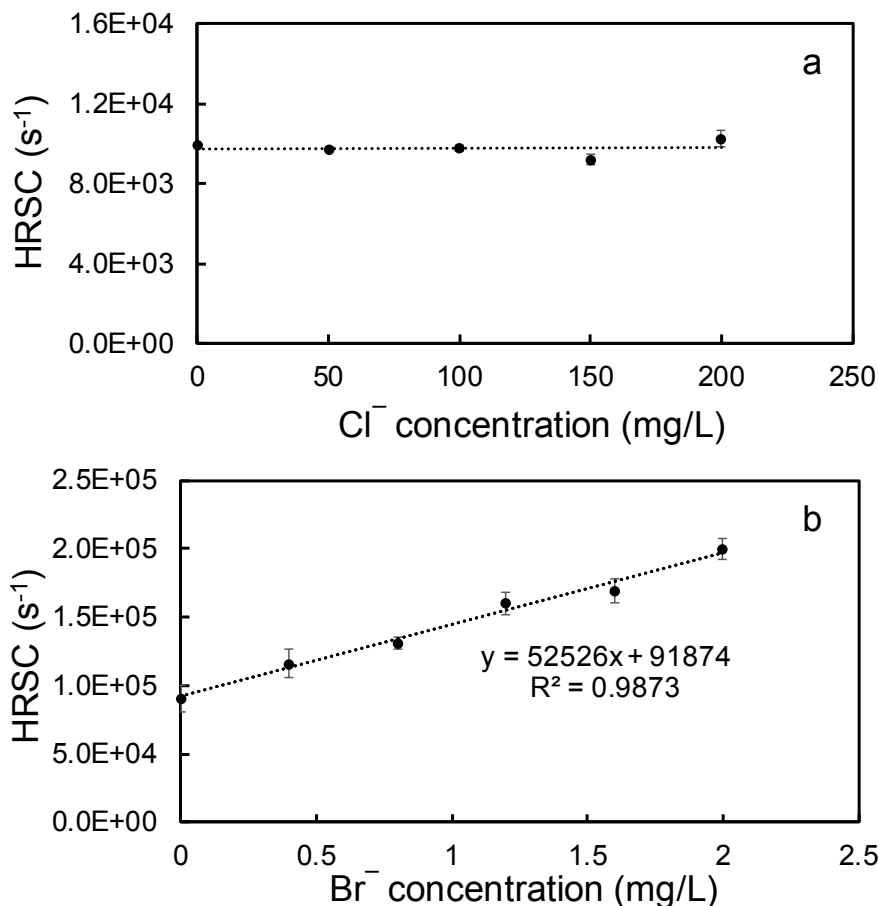
317 The addition of chloride to tap water samples at doses up to 200 mg/L had no significant impact
318 on scavenging capacity, which remained close to that before chloride spiking (Fig. 5a). This is
319 consistent with previous findings that chloride has limited impact on the UV/H₂O₂ process.²⁴
320 Although chloride reacts fast with hydroxyl radical (Eq. 7), the reverse reaction is also fast at pH
321 levels relevant to water treatment (Eq. 8), generating the •OH back through instant disintegration
322 of the product from Eq. 7. The net result is the negligible HRSC from chloride.^{25, 26} The
323 contribution of chlorine radical is not relevant here. Once ClOH•⁻ is formed, further generation of
324 chlorine radicals requires its protonation to form ClOH₂•. This intermediate can then lose H₂O to
325 produce Cl•. However, this pathway requires a pH below 4.²⁷





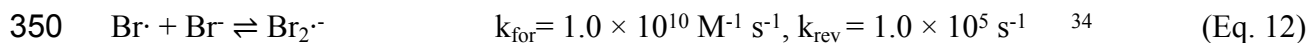
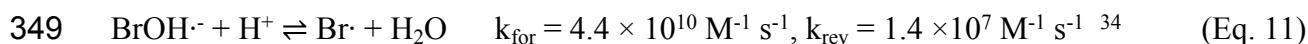
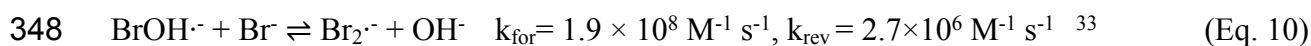
328 Different concentrations of bromide were added to tap water samples to investigate its effect on
329 measuring HRSC. The results showed a significant influence of bromide at mg/L levels on HRSC
330 of water samples (Fig. 5b), with $5.4 \times 10^4 \text{ s}^{-1}$ HRSC increase for each mg/L Br^- concentration
331 increase. By Eq.1 with bromide's reaction rate constant with $\bullet\text{OH}$ of $1.1 \times 10^{10} \text{ M}^{-1} \text{ s}^{-1}$,²⁵ the
332 theoretical HRSC of 1 mg/L of bromide was calculated to be $1.4 \times 10^5 \text{ s}^{-1}$, which is higher than the
333 experimentally observed value of $5.4 \times 10^4 \text{ s}^{-1}$. This can be attributed to reversible reaction shown
334 in Eq. 9, in which $\text{BrOH}^{\bullet-}$ rapidly dissociates to regenerate $\bullet\text{OH}$. Meanwhile, $\text{BrOH}^{\bullet-}$ can react
335 with Br^- to form $\text{Br}_2^{\bullet-}$ (Eq. 10) or go through proton-assisted dissociation (Eq. 11) to generate
336 $\text{Br}^{\bullet-}$, followed by conversion into $\text{Br}_2^{\bullet-}$ through Eq. 12. Both $\text{Br}^{\bullet-}$ and $\text{Br}_2^{\bullet-}$ are highly selective
337 radicals that primarily react with electron-rich species.²⁸ Therefore, converting hydroxyl radicals
338 into less reactive bromine radicals increases HRSC and compromises AOP performance, as
339 reported by Zhang and Parker.²⁹ Although in most natural water bromide concentrations do not
340 exceed 0.5 mg/L,³⁰ some surface waters in Israel and Australia were reported to have
341 concentrations up to 2-4 mg/L,^{31,32} making bromide a major $\bullet\text{OH}$ scavenger.





342
343 Fig. 5 HRSC of tap water in the presence of a) chloride and b) bromide (TOC = 4.3 mg-C/L, pH
344 = 7.1) at room temperature. The error bars indicate the maximum and minimum values from
345 duplicate tests.

346



351 Another potential interference of bromide on HRSC measurement is the catalytic decay of H₂O₂

352 by bromide.³⁵ If H₂O₂ decay is significantly accelerated by the presence of bromide, the



353 assumption of constant $\bullet\text{OH}$ production in the external calibration method would be invalid. Under
354 our test conditions, we found that such a catalytical effect on H_2O_2 decay is negligible as shown
355 in Fig. S3, which shows similar decay rates of H_2O_2 with and without bromine over the six
356 minutes' test time.

357 3.3 Effect of chloramines on the scavenging capacity measurement

358 HRSC measurement is complicated by the presence of chloramines in water samples, such as RO
359 permeates in water reuse where residuals of chloramines added upstream for membrane fouling
360 control is present. Although the scavenging capacity of chloramines can be combined with the
361 intrinsic scavenging capacity of the original water samples and measured as a single total value,
362 the interpretation of this total may be confounded by the additional $\bullet\text{OH}$ generated through
363 chloramine photolysis. This extra radical production violates the key assumption of the external
364 calibration method—the hydroxyl radical generation rate remains constant. Fig. 6 demonstrates
365 the effect of chloramines on the HRSC in simulated RO which has an initial HRSC of $1.1 \times 10^4 \text{ s}^{-1}$.
366 By adding chloramines at 2-4 $\text{mg-Cl}_2/\text{L}$, which were a mixture of monochloramine and
367 dichloramine (Fig. S4), to the water matrix, the scavenging capacity increased to about 4 to 8×10^4
368 s^{-1} . When the chloramine concentration exceeded 5 $\text{mg-Cl}_2/\text{L}$, the HRSC showed a diminishing
369 increase, probably because of the generation of $\bullet\text{OH}$ by chloramine photolysis which compensates
370 for the consumption of $\bullet\text{OH}$. Therefore, the true scavenging capacity caused by chloramines,
371 which, by definition, is only determined by the chloramines' concentrations and reactivities toward
372 hydroxyl radical, should be higher than that measured by the external calibration method (Fig. 6).
373 Another challenge in measuring the HRSC of chloramine-containing water is the instability of
374 chloramines. Their concentration and speciation can change during UV-AOPs, sample shipping,

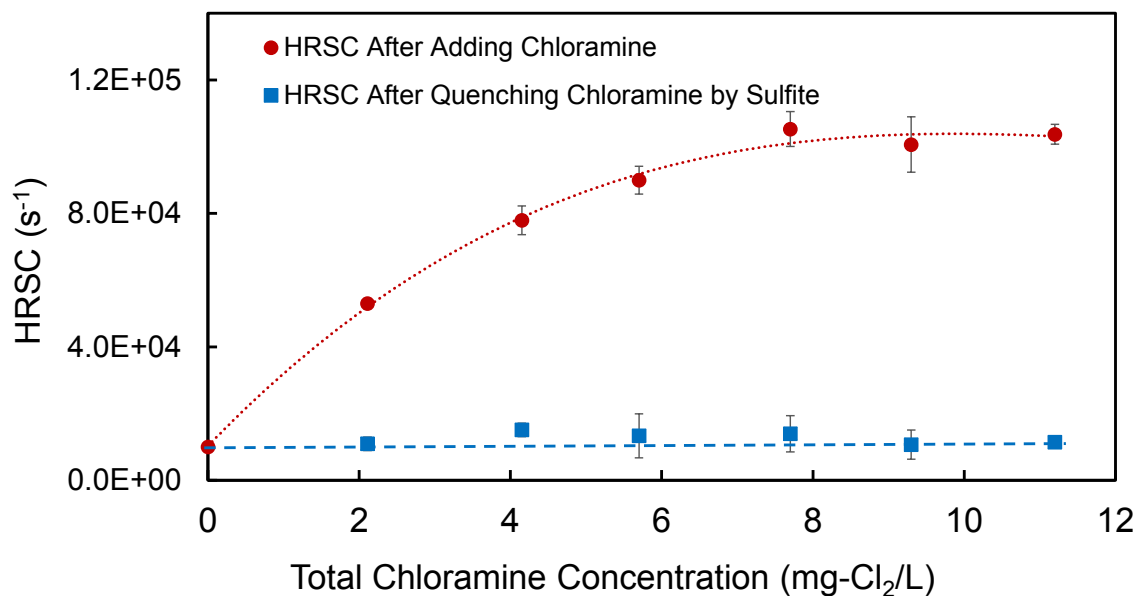


375 and storage, which leads to uncertainties of experimentally measured HRSCs and their relevance
376 to process optimization. Therefore, it is advisable to quench chloramines prior to HRSC
377 measurement so that the measured HRSC represents the background value (HRSC_b). The HRSC
378 by chloramines (HRSC_c) can then be calculated or modelled from their concentrations and
379 corresponding rate constants. The total HRSC (HRSC_t) is thus the sum of HRSC_b and HRSC_c (Eq.
380 13).

$$381 \quad \text{HRSC}_t = \text{HRSC}_b + \text{HRSC}_c \quad (\text{Eq. 13})$$

382 Therefore, common chloramine quenching agents, sulfite/bisulfite, were tested for their suitability
383 for such purpose. As shown in Fig. 6, when sulfite was added to water samples to
384 stoichiometrically quench chloramines at a sulfite/Cl molar ratio of 1:1, the HRSC of the water
385 samples was restored to approximately $(1.3 \pm 0.2) \times 10^4 \text{ s}^{-1}$, which is close to its level before adding
386 chloramines ($(1.1 \pm 0.2) \times 10^4 \text{ s}^{-1}$). This indicates that sulfite is an effective chloramine quenching
387 agent without changing the original HRSC of the water samples. This is because the products of
388 the quenching reaction, ammonium and chloride, have negligible HRSC under these conditions
389 due to their low concentrations and low reactivity towards $\bullet\text{OH}$.^{26, 36}





390
391 Fig. 6 HRSC before and after quenching chloramine using sodium sulfite in simulated RO at
392 room temperature (TOC < 0.3 mg-C/L; initial pH was 5.5, and after chloramine quenching, it
393 increased to 5.8-5.9). The error bars indicate the maximum and minimum values from duplicate
394 tests.

395 Sodium bisulfite is as effective as sodium sulfite in quenching chloramines and restoring the HRSC
396 to the levels before the addition of chloramine, as seen in Fig. S5. However, sodium sulfite is
397 preferred over sodium bisulfite, because sodium bisulfite decreases the water pH, for example,
398 from an initial pH of 5.5 to 3.8 at a dose of 5.8 mg/L of NaHSO₃. This unusually low pH may alter
399 the molecular structure of MB and even its reactivity toward •OH, as implied by the slightly higher
400 MB absorbance at pH 2–4 compared with near-neutral pH (Fig. S6). It is possible that such a low
401 pH may invalidate the calibration curve, although further research is needed to investigate this.
402 MB has a reported pK_a of ~3.8,³⁷ and near this pH protonation can alter its molecular structure
403 and, consequently, its optical properties. Thus, changes in MB's optical response are expected
404 primarily under acidic conditions, with minimal effects at higher pH.

405 Precise quenching of chloramines can be challenging, particularly during on-site sample
406 collection. In such cases, excess sulfite is often preferred and sometimes unavoidable. Provided



407 that the excess sulfite is counter-quenched by H₂O₂ prior to HRSC analysis, which may take half
408 an hour or longer depending on concentrations and pH,³⁸ the sample's HRSC can be restored to its
409 background values and measured with high reliability. However, the long-term (e.g., days or
410 weeks) effect of excess sulfite on samples' HRSC during sample shipping and storage has not been
411 investigated.

412 4. Conclusion

413 This study investigated potential interferences in the external calibration method for measuring
414 HRSC of water samples. Our results indicated that carbonate radical, superoxide radical, organic
415 radicals and singlet oxygen exhibited no detectable reactions towards MB within the typical HRSC
416 measurement time, confirming that the decay of MB is solely attributable to its reaction with
417 hydroxyl radicals and validating its suitability as a •OH probe. Chloride showed no effect on HRSC
418 at concentrations up to 200 mg/L, whereas bromide at mg/L levels significantly increased HRSC.
419 Chloramines, an oxidant commonly present in RO permeate prior to UV-AOP treatment, can
420 contribute substantially to the measured HRSC. However, experimentally quantifying their
421 contribution is challenging because chloramines also generate hydroxyl radicals under UV
422 irradiation, and their concentration is typically unstable in UV AOPs and during shipping and
423 storage, making measurement inaccurate. Therefore, we recommend quenching chloramines
424 stoichiometrically with sulfite. HRSC contribution by chloramines can then be calculated based
425 on chloramine concentrations and the corresponding hydroxyl-radical reaction rate constants.
426 Overall, this work supports the robust application of the external calibration method in most
427 drinking water systems and helps reduce uncertainty in measuring HRSC and optimizing UV-AOP
428 operation. The feasibility of this method in other water matrices, such as wastewater with extreme



429 pH or ionic strength levels, high metal concentrations, and high particle concentration, warrants
430 further investigation.

431 **CRedit authorship contribution statement**

432 Fateme Mohamadi: investigation, data analysis, and original draft. Tianyi Chen: review and
433 editing, funding acquisition. Ron Hofmann: conceptualization, funding acquisition, review and
434 editing. Chengjin Wang: conceptualization, funding acquisition, review & editing.

435 **Acknowledgments**

436 The authors acknowledge the financial support provided by the following funding organizations:
437 the Water Research Foundation (Project No. 5194) and the California State Water Resources
438 Control Board, the University Research Grants Program (URGP) at the University of Manitoba
439 (Project No. 59860), and the New Investigator Operating Grant sponsored by Research Manitoba.
440 This material does not necessarily reflect the views and policies of the funders.

441 **Declaration of competing interest:**

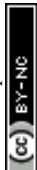
442 Authors declare that there are no competing financial interests or personal relationships with other
443 people or funding organizations which have influenced their work.

444 **References**

- 445 1. E. J. Rosenfeldt and K. G. Linden, The $R_{OH,UV}$ concept to characterize and the model
446 UV/H₂O₂ process in natural waters, *Environ. Sci. Technol.*, 2007, 41, 2548-2553.
- 447 2. C. Wang, E. Rosenfeldt, Y. Li and R. Hofmann, External standard calibration method to
448 measure the hydroxyl radical scavenging capacity of water samples, *Environ. Sci.*
449 *Technol.*, 2020, 54, 1929-1937.
- 450 3. Y. Liu, X. He, X. Duan, Y. Fu, D. Fatta-Kassinos and D. D. Dionysiou, Significant role
451 of UV and carbonate radical on the degradation of oxytetracycline in UV-AOPs: Kinetics
452 and mechanism, *Water Res.*, 2016, 95, 195-204.
- 453 4. E. Tsui, H. Wang and R. R. Knowles, Catalytic generation of alkoxy radicals from
454 unfunctionalized alcohols, *Chem. Sci.*, 2020, 11, 11124-11141.



- 455 5. Z. Luo, Y. Yan, R. Spinney, D. D. Dionysiou, F. A. Villamena, R. Xiao and D. Vione,
456 Environmental implications of superoxide radicals: From natural processes to
457 engineering applications, *Water Res.*, 2024, 261, 122023.
- 458 6. L. A. C. Teixeira, M. T. C. Arellano, C. Marquez Sarmiento, L. Yokoyama and F. V. d.
459 F. Araujo, Oxidation of cyanide in water by singlet oxygen generated by the reaction
460 between hydrogen peroxide and hypochlorite, *Miner. Eng.*, 2013, 50-51, 57-63.
- 461 7. M. Kwon, A. Royce, Y. Gong, K. P. Ishida and M. I. Stefan, UV/chlorine vs. UV/H₂O₂
462 for water reuse at Orange County Water District, CA: a pilot study, *Environ. Sci.: Water
463 Res. Technol.*, 2020, 6, 2416-2431.
- 464 8. D. L. McCurry, K. P. Ishida, G. L. Oelker and W. A. Mitch, Reverse osmosis shifts
465 chloramine speciation causing re-formation of NDMA during potable reuse of
466 wastewater, *Environ. Sci. Technol.*, 2017, 51, 8589-8596.
- 467 9. Y. Li, W. Song, W. Fu, D. C. W. Tsang and X. Yang, The roles of halides in the
468 acetaminophen degradation by UV/H₂O₂ treatment: Kinetics, mechanisms, and products
469 analysis, *Chem. Eng. J.*, 2015, 271, 214-222.
- 470 10. G. V. Buxton, C. L. Greenstock, W. P. Helman and A. B. Ross, Critical review of rate
471 constants for reactions of hydrated electrons, hydrogen atoms and hydroxyl radicals
472 ($\cdot\text{OH}/\cdot\text{O}^-$) in aqueous solution, *J. Phys. Chem. Ref. Data*, 1988, 17, 513-886.
- 473 11. J. C. Crittenden, R. R. Trussell, D. W. Hand, K. J. Howe and G. Tchobanoglous, *MWH's
474 water treatment: principles and design*, Wiley, New Jersey, 2012.
- 475 12. K. Sehested, J. Holcman, E. Bjergbakke and E. J. Hart, Ozone decomposition in aqueous
476 acetate solutions, *J. Phys. Chem.*, 1987, 91, 2359-2361.
- 477 13. N. Moore, C. Wang, S. Andrews and R. Hofmann, On the increasing competitiveness of
478 UV/Cl to UV/H₂O₂ advanced oxidation as the organic carbon concentration increases,
479 *Water Res.*, 2023, 242, 120227.
- 480 14. B. Velika and I. Kron, Antioxidant properties of benzoic acid derivatives against
481 superoxide radical, *Free Radic. Antioxid.*, 2012, 2, 62-67.
- 482 15. J. K. Hurst, P. A. G. Carr, F. E. Hovis and R. J. Richardson, Hydrogen peroxide oxidation
483 by chlorine compounds. Reaction dynamics and singlet oxygen formation, *Inorg. Chem.*,
484 1981, 20, 2435-2438.
- 485 16. E. Appiani, R. Ossola, D. E. Latch, P. R. Erickson and K. McNeill, Aqueous singlet
486 oxygen reaction kinetics of furfuryl alcohol: effect of temperature, pH, and salt content,
487 *Environ. Sci.: Processes Impacts*, 2017, 19, 507-516.
- 488 17. N. V. Klassen, D. Marchington and H. C. E. McGowan, H₂O₂ determination by the I₃⁻
489 method and by KMnO₄ titration, *Anal. Chem.*, 1994, 66, 2921-2925.
- 490 18. A. D. Eaton, M. A. H. Franson, A. P. H. Association, A. W. W. Association and W. E.
491 Federation, *Standard methods for the examination of water & wastewater*, American
492 Public Health Association, 2005.
- 493 19. L. Wojnárovits, T. Tóth and E. Takács, Rate constants of carbonate radical anion
494 reactions with molecules of environmental interest in aqueous solution: A review, *Sci.
495 Total Environ.*, 2020, 717, 137219.
- 496 20. S. Yang, S. Sun, Z. Xie, Y. Dong, P. Zhou, J. Zhang, Z. Xiong, C.-S. He, Y. Mu and B.
497 Lai, Comprehensive insight into the common organic radicals in advanced oxidation
498 processes for water decontamination, *Environ. Sci. Technol.*, 2024, 58, 19571-19583.
- 499 21. L. Bai, L. He, Y. Fu, C. Chu, Z. Wei, R. Spinney, D. D. Dionysiou, Y. Liang and R.
500 Xiao, New insight to superoxide radical-mediated degradation of pentachlorophenate:



- 501 Kinetic determination and theoretical calculations, *Chem. Commun.*, 2022, 58, 2666-
502 2669.
- 503 22. Q. V. Vo, L. T. T. Thao, T. D. Manh, M. V. Bay, B.-T. Truong-Le, N. T. Hoa and A.
504 Mechler, Reaction of methylene blue with OH radicals in the aqueous environment:
505 mechanism, kinetics, products and risk assessment, *RSC Adv.*, 2024, 14, 27265-27273.
- 506 23. W. R. Haag, J. r. Hoigne, E. Gassman and A. M. Braun, Singlet oxygen in surface waters
507 — Part I: Furfuryl alcohol as a trapping agent, *Chemosphere*, 1984, 13, 631-640.
- 508 24. W. Zhang, S. Zhou, J. Sun, X. Meng, J. Luo, D. Zhou and J. Crittenden, Impact of
509 chloride ions on UV/H₂O₂ and UV/persulfate advanced oxidation processes, *Environ. Sci.*
510 *Technol.*, 2018, 52, 7380-7389.
- 511 25. J. E. Grebel, J. J. Pignatello and W. A. Mitch, Effect of halide ions and carbonates on
512 organic contaminant degradation by hydroxyl radical-based advanced oxidation processes
513 in saline waters, *Environ. Sci. Technol.*, 2010, 44, 6822-6828.
- 514 26. J. Fang, Y. Fu and C. Shang, The roles of reactive species in micropollutant degradation
515 in the UV/free chlorine system, *Environ. Sci. Technol.*, 2014, 48, 1859-1868.
- 516 27. L. Wojnárovits and E. Takács, Rate constants of dichloride radical anion reactions with
517 molecules of environmental interest in aqueous solution: a review, *Environ. Sci. Pollut.*
518 *Res. Int.*, 2021, 28, 41552-41575.
- 519 28. Y. Lei, X. Lei, P. Westerhoff, X. Tong, J. Ren, Y. Zhou, S. Cheng, G. Ouyang and X.
520 Yang, Bromine radical (Br• and Br₂•⁻) reactivity with dissolved organic matter and
521 brominated organic byproduct formation, *Environ. Sci. Technol.*, 2022, 56, 5189-5199.
- 522 29. K. Zhang and K. M. Parker, Halogen radical oxidants in natural and engineered aquatic
523 systems, *Environ. Sci. Technol.*, 2018, 52, 9579-9594.
- 524 30. World Health Organization, Bromide in drinking-water : background document for
525 development of WHO guidelines for drinking-water quality, 2009.
- 526 31. A. Wang, Z. Hua, Z. Wu, C. Chen, S. Hou, B. Huang, Y. Wang, D. Wang, X. Li, C. Li
527 and J. Fang, Insights into the effects of bromide at fresh water levels on the radical
528 chemistry in the UV/peroxydisulfate process, *Water Res.*, 2021, 197, 117042.
- 529 32. R. S. Magazinovic, B. C. Nicholson, D. E. Mulcahy and D. E. Davey, Bromide levels in
530 natural waters: its relationship to levels of both chloride and total dissolved solids and the
531 implications for water treatment, *Chemosphere*, 2004, 57, 329-335.
- 532 33. I. Lampre, J.-L. Marignier, M. Mirdamadi-Esfahani, P. Pernot, P. Archirel and M.
533 Mostafavi, Oxidation of bromide ions by hydroxyl radicals: spectral characterization of
534 the intermediate BrOH•⁻, *J. Phys. Chem. A*, 2013, 117, 877-887.
- 535 34. Y. Xue, Z. Wang, R. Naidu, R. Bush, F. Yang, J. Liu and M. Huang, Role of halide ions
536 on organic pollutants degradation by peroxygens-based advanced oxidation processes: A
537 critical review, *Chem. Eng. J.*, 2022, 433, 134546.
- 538 35. W. C. Bray and R. S. Livingston, The catalytic decomposition of hydrogen peroxide in a
539 bromine-bromide solution, and a study of the steady state, *J. Am. Chem. Soc.*, 1923, 45,
540 1251-1271.
- 541 36. X. Yang, Y. Tao and J. G. Murphy, Kinetics of the oxidation of ammonia and amines
542 with hydroxyl radicals in the aqueous phase, *Environ. Sci.: Processes Impacts*, 2021, 23,
543 1906-1913.
- 544 37. J. J. Salazar-Rabago, R. Leyva-Ramos, J. Rivera-Utrilla, R. Ocampo-Perez and F. J.
545 Cerino-Cordova, Biosorption mechanism of methylene blue from aqueous solution onto



- 546 white pine (*Pinus durangensis*) sawdust: Effect of operating conditions, *Sustain. Environ.*
547 *Res.*, 2017, 27, 32-40.
548 38. C. Wang, M. Hofmann, A. Safari, I. Viole, S. Andrews and R. Hofmann, Chlorine is
549 preferred over bisulfite for H₂O₂ quenching following UV-AOP drinking water treatment,
550 *Water Res.*, 2019, 165, 115000.

551

552



Data Availability

View Article Online
DOI: 10.1039/D6EW00171H

The data supporting this article have been included as part of the supplementary information (SI). Supplementary information is available.

